Design and Fabrication of Zwitter-Wettable Nanostructured Films

Hyomin Lee,[†,⊥] Jonathan B. Gilbert,[†,⊥] Francesco E. Angilè,[‡] Rong Yang,[†] Daeyeon Lee,[‡] Michael F. Rubner,*[,§] and Robert E. Cohen*[,†]

[†]Department of Chemical Engineering, Massachusetts Institute of Technology, Cambridge, Massachusetts 02139, United States

[‡]Department of Chemical and Biomolecular Engineering, University of Pennsylvania, Philadelphia, Pennsylvania 19104, United States

[§]Department of Materials Science and Engineering, Massachusetts Institute of Technology, Cambridge, Massachusetts 02139, United States

Ⓢ Supporting Information

ABSTRACT: Manipulating surface properties using chemistry and roughness has led to the development of advanced multifunctional surfaces. Here, in a nanostructured polymer film consisting of a hydrophilic reservoir of chitosan/ carboxymethyl cellulose capped with various hydrophobic layers, we demonstrate the role of a third design factor, water permeation rate. We use this additional design criterion to produce antifogging coatings that readily absorb water vapor while simultaneously exhibiting hydrophobic character to liquid

water. These zwitter-wettable films, produced via aqueous layer-by-layer assembly, consist of a nanoscale thin hydrophobic capping layer (chitosan/Nafion) that enables water vapor to diffuse rapidly into the underlying hydrophilic reservoir rather than nucleating drops of liquid water on the surface. We characterize these novel films using a quartz crystal microbalance with dissipation monitoring (QCM-D) and via depth-profiling X-ray photoelectron spectroscopy (XPS) in addition to extensive testing for fogging/antifogging performance.

KEYWORDS: wetting, zwitter-wettability, layer-by-layer, condensation, surface science, antifogging coatings
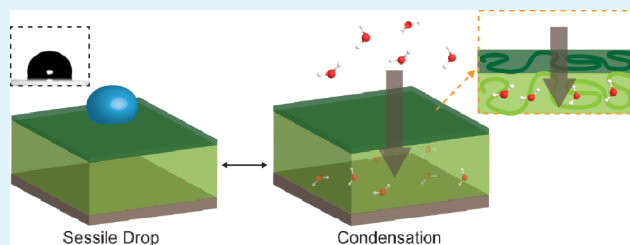
1. INTRODUCTION

Smooth hydrophilic[1] or nanotextured superhydrophilic surfaces[2−4] are often used to control water condensation and produce antifogging coatings. This is typically accomplished by facilitating the condensation of a thin film of optically clear water.[1,5] However, it was recently demonstrated by us[6] and others[7] that effective antifog and antifrost coatings can also be hydrophobic. These counterintuitive polymeric systems consist of hydrophilic and hydrophobic moieties that can directly imbibe water molecules from the vapor phase into the film, while the surface maintains a hydrophobic character. We recently defined these coatings as zwitter-wettable[6] films (also reported by others as hydrophobic but hygroscopic films[8]), due to the capability to simultaneously absorb water vapor from the environment while exhibiting hydrophobic character to water droplets.

The initial system we investigated was fabricated using layer-by-layer (LbL) assembly of partially hydrolyzed poly(vinyl alcohol) (PVA) and poly(acrylic acid) (PAA).[9] Although hydrophobic acetate moieties of PVA are required to enable LbL assembly, these hydrophobic acetate groups resulted in the observation of abnormally high water contact angles (as high as 110°[6]) that was also accompanied by a significant hydrophobic to hydrophilic surface rearrangement when probed with water droplets (in the condensed liquid state).[6,10] This transient contact angle behavior may be undesirable in specific

applications and makes characterization of the wetting behavior more difficult.

In this work, we demonstrate that zwitter-wettable polymer systems can be fabricated such that the surface hydrophobicity does not decay with time. These new systems are used to provide general design criteria for creating zwitter-wettable films. Specifically, we show that a hydrophilic reservoir capped with a very thin hydrophobic layer with high water permeability can be used to limit the nucleation and growth of water droplets on a surface during condensation and thereby produce antifogging coatings with nontransient zwitter-wettable characteristics.

2. EXPERIMENTAL SECTION

2.1. Layer-by-Layer Assembly of the Polymer Thin Films. Sequential adsorption of polymer layers were performed using a StratoSequence VI spin dipper (nanoStrata Inc.), controlled by StratoSmart v6.2 software, at 80 rpm. The concentrations of chitosan (CHI, low molecular weight), carboxymethylcellulose (CMC, Mw = 250 000 g/mol) and Nafion dispersion (Alfa Aesar, 5% (w/w) in water and 1-propanol) in the dipping solutions were 1 mg/mL, 1 mg/mL and 0.25% (w/w), respectively. For chitosan, 0.3% (v/v) acetic acid was added prior to dissolving the polymer and was filtered with 200 μm pore filter (VWR) after stirring overnight. Distilled water (>18
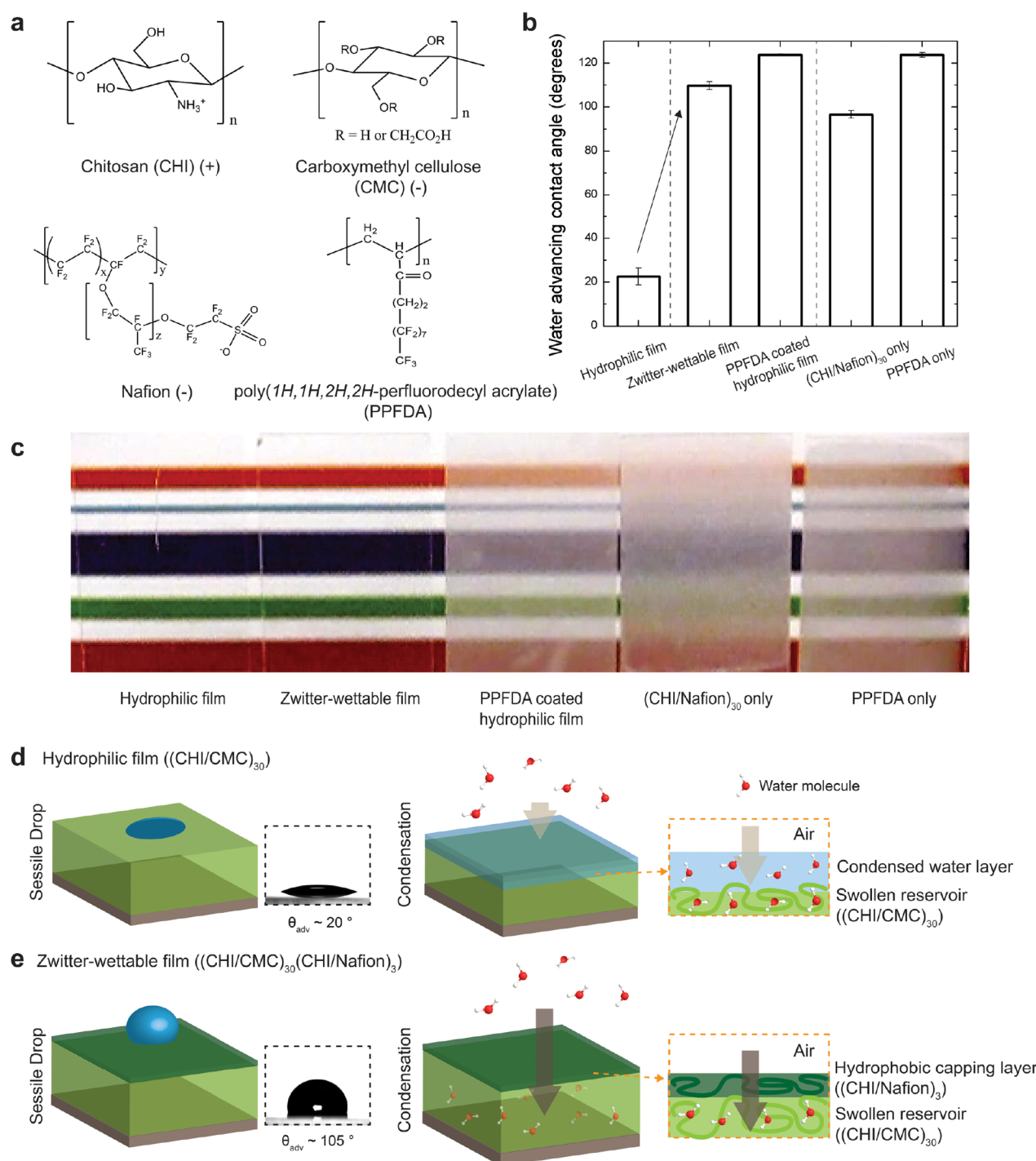
Figure 1. (a) Structures of the polymers described in this paper. Polycations and polyanions are labeled with parentheses (+), (−), respectively. (b) Water advancing contact angles of the samples tested. (c) Photographs of glass slides with different coatings placed in front of a striped design taken immediately after transfer to ambient lab conditions (22 ± 1 °C, 40 ± 10% RH) from a −1 °C refrigerator (1 h). Only the hydrophilic film and zwitter-wettable film resisted fog formation. Here, "hydrophilic film" refers to 30 bilayer LbL assembled multilayer film of CHI/CMC while "zwitter-wettable film" is the same film with addition of three bilayers of (CHI/Nafion) on top. (d) Schematic representation of a hydrophilic film with added sessile drop and during condensation. (e) Schematic representation of a zwitter-wettable film with added sessile drop and during condensation.

MΩ·m, Millipore Milli-Q) (DI water) was used in formulating the solution and in all rinsing procedures. The dipping times in the CHI, CMC and Nafion solutions were each 10 min followed by three sequential rinse steps (of 2, 1 and 1 min). All solutions and their respective rinse solutions were adjusted to pH 4.0 with either NaOH or HCl, respectively.

Glass substrates were first degreased by sonication in a 4% (v/v) solution of Micro-90 cleaner (International Products Co.) for 15 min,

subsequently sonicated twice in DI water for 15 min. The substrates were blow-dried with dry air and treated for 2 min with oxygen plasma (PDC-32G, Harrick Scientific Products, Inc.) at 150 mTorr before the LbL assembly.

2.2. Contact Angle Measurements. Transient contact angle measurements as well as advancing and receding contact angles of probe liquids on various samples were performed using a Ramé-Hart

Table 1. Thickness of the Multilayer Films Assembled on Glass Substrate

$(CHI/CMC)_{30}$	$(CHI/CMC)_{30}(CHI/Nafion)_3$	$(CHI/CMC)_{30}$ PPFDA	$(CHI/Nafion)_{30}$ only	PPFDA only
615 ± 16 nm	684 ± 5 nm (+ 69 nm)[a]	677 ± 1 nm (+ 62 nm)[a]	18 ± 3 nm	72 ± 2 nm

[a]Film thickness change after deposition of a hydrophobic capping layer.

model 590 goniometer, by dispensing liquid droplets of volume $V \sim 10 \ \mu L$.

2.3. Preparation of Poly(1H,1H,2H,2H-perfluorodecyl acrylate) (PPFDA) Coating Using Initiated Chemical Vapor Deposition (iCVD). iCVD polymerization of 1H,1H,2H,2H-perfluorodecyl acrylate (PFDA) (97%, Aldrich) was conducted as previously described.[11] Briefly, the peroxide initiator, tert-butyl peroxide (TBPO) (98%, Aldrich), was delivered into the reactor through a mass flow controller (MKS Instruments) at a constant flow rate. PFDA was vaporized in a glass jar that was heated to 80 °C. The flow rate was controlled using a needle valve and kept constant at 0.6 sccm. The nickel−chromium filaments (Goodfellow) were resistively heated to 290 °C using a DC power supply (Sorensen), and the temperature was measured by a K-type thermocouple (Omega Engineering). The sample stage was cooled at 40 °C using a recirculating chiller/heater (NESLAB). The working pressure was maintained at 200 mTorr using a throttling valve (MKS Instruments). The reactor was covered with a quartz top (2.5 cm) that allows in situ thickness monitoring by interferometry with a 633 nm HeNe laser source (JDS Uniphase). The final thickness of the polymer layer deposited on top of the hydrophilic film corresponds to 62 nm.

2.4. Permeability Measurements Using Quartz Crystal Microbalance with Dissipation Monitoring (QCM-D). Gold-coated QCM-sensors (Q-Sense Inc.) are cleaned with oxygen plasma and piranha treatment using previously published protocols.[12] *Caution!* Piranha solution is aggressive and explosive. Never mix piranha waste with solvents. Check the safety precautions before using it. The baseline frequency and dissipation are first recorded with a blank crystal under dry nitrogen and calibrated to zero for the sorption measurements. All the multilayer films are then formed on the crystals through the similar procedure used for glass substrate. Here, gold crystals were immobilized on a plastic microscope slide (P11011P) in between two grooves made with a razor blade. The film on the back side of crystal is carefully removed using 1.0 M NaOH with a cotton swab and then rinsed thoroughly with DI water. After the multilayer coated sensors are loaded in the QCM chamber (E4 QCM-D unit (Q-Sense Inc.)), the frequency and dissipation shifts are monitored at varying humidity conditions.

The measured frequency and dissipation are fitted using the Voigt viscoelastic model incorporated in Q-Sense analysis software (QTools) to calculate the transient increase in film thickness that occurs as a result of permeation of water vapor into the film following a step change in relative humidity from 30% RH to 60% RH. Details of this procedure have been described previously.[12] The average density of chitosan, carboxymethyl cellulose and Nafion was used to determine the film thickness from QCM-D measurements.

2.5. Scanning Electron Microscopy (SEM) Measurements. Scanning electron microscopy (SEM) micrographs were obtained using a JEOL 6010LA in back scattered electron shadow image mode (BES) operated at an accelerating voltage of 10 kV. Energy dispersive X-ray spectrometry (EDS) was performed as well to perform elemental analysis of the zwitter-wettable patch sample. Environmental scanning electron microscope (ESEM, Zeiss Evo 55) was used to investigate the nucleation and condensation phenomena in situ.

2.6. Depth Profiling X-ray Photoelectron Spectroscopy. Chemical composition of the surface was characterized using a PHI Versaprobe II X-ray photoelectron spectrometer with a scanning monochromated Al source (1486.6 eV, 50W, spot size 200 um). Depth profiling was accomplished using the instrument's C_{60}^+ ion source. The takeoff angle between the sample surface and analyzer was 45° and the X-ray beam collected C_{1s}, O_{1s}, F_{1s}, N_{1s} and Si_{2p} elemental information while rastering over a $200 \times 350 \ \mu m$ area. Detailed XPS acquisition parameters are in the Supporting Information (Table S1). Sputtering occurred in 1 min intervals while the sample was moved

using concentric Zalar rotation at 1 rpm. The C_{60}^+ source was operated at 10 kV and 10 nA and rastered over a 3×3 mm area at an angle 70° to the surface normal. Atomic composition was determined based on photoelectron peak areas and the relative sensitivity factors provided in PHI's Multipak processing software. All data were background subtracted, smoothed using a five point quadratic Savitzky−Golay (S-G) algorithm and charge-corrected so that the carbon−carbon bond has a binding energy of 285.0 eV. The surface of the glass substrate was defined as the point at which the atomic concentration of silicon reached 5% in the depth profiling data. The molar repeat unit ratio profile was calculated via an oxygen mass balance and to minimize experimental bias, pure films of chitosan, CMC, Nafion and PPFDA were analyzed via depth profiling XPS as the basis for the effective molecular repeats.

2.7. Zwitter-Wettable Patch Fabrication. Patch fabrication was based on a photolithographic lift off procedure. Briefly, the slides were cleaned with 2% (v/v) solution of Micro-90 cleaner (International Products Co.), 1 M NaOH and then rinsed with water. Next, the photoresist was spin coated onto the surface and developed as previously described.[13] After deposition of the uniform hydrophilic layer via layer-by-layer processing, the film was patterned by dissolving the remaining photoresist in sonicating acetone for 10 s, leaving behind patches of hydrophilic (CHI/CMC). Finally the hydrophobic (CHI/Nafion) film was deposited uniformly over the surface via layer-by-layer processing.

3. RESULTS AND DISCUSSION

3.1. Fabrication of Zwitter-Wettable Films. LbL assembly was utilized to produce various films with heterostructured architectures.[14] For the base platform, we used hydrophilic polysaccharides (chitosan (CHI) as the polycation (+) and carboxymethyl cellulose (CMC) as the polyanion (−)), as shown in Figure 1a; this hydrophilic film has good antifogging properties, as reported earlier.[1] As shown in Figure 1b, a 30 bilayer coating of CHI/CMC on a glass substrate exhibits water advancing contact angle of ∼20°. The surface wetting characteristics of this 30 bilayer hydrophilic antifogging film were modified to exhibit hydrophobic behavior by two different methods: (a) the addition of three LbL bilayers of (CHI/Nafion) or (b) by chemical vapor deposition (CVD) of poly(1H,1H,2H,2H-perfluorodecyl acrylate) (PPFDA). The three bilayers of CHI/Nafion increased the water advancing contact angle to ∼110° whereas the PPFDA coating increased the water advancing contact angle to ∼125°. At least three bilayers of (CHI/Nafion) were needed to prevent transient contact angle behavior due to surface rearrangement.[10] Thus, all samples investigated contained at least three (CHI/Nafion) bilayers and did not exhibit any significant time dependent contact angles (Supporting Information, Figure S1).

To test for antifog capability, photographs of samples were taken immediately after transfer to ambient lab conditions (22 ± 1 °C, 40 ± 10% RH) from a −1 °C refrigerator (1 h incubation time). As shown in Figure 1c, only the standard hydrophilic film ($(CHI/CMC)_{30}$) and a CHI/Nafion coated hydrophilic film ($(CHI/CMC)_{30}(CHI/Nafion)_3$) resisted fog formation during this fogging challenge. It has been reported earlier[1] that the hydrophilic CHI/CMC film remains optically clear during condensation due to its strong water-absorbing characteristics that enable the formation of a uniform, nonlight-
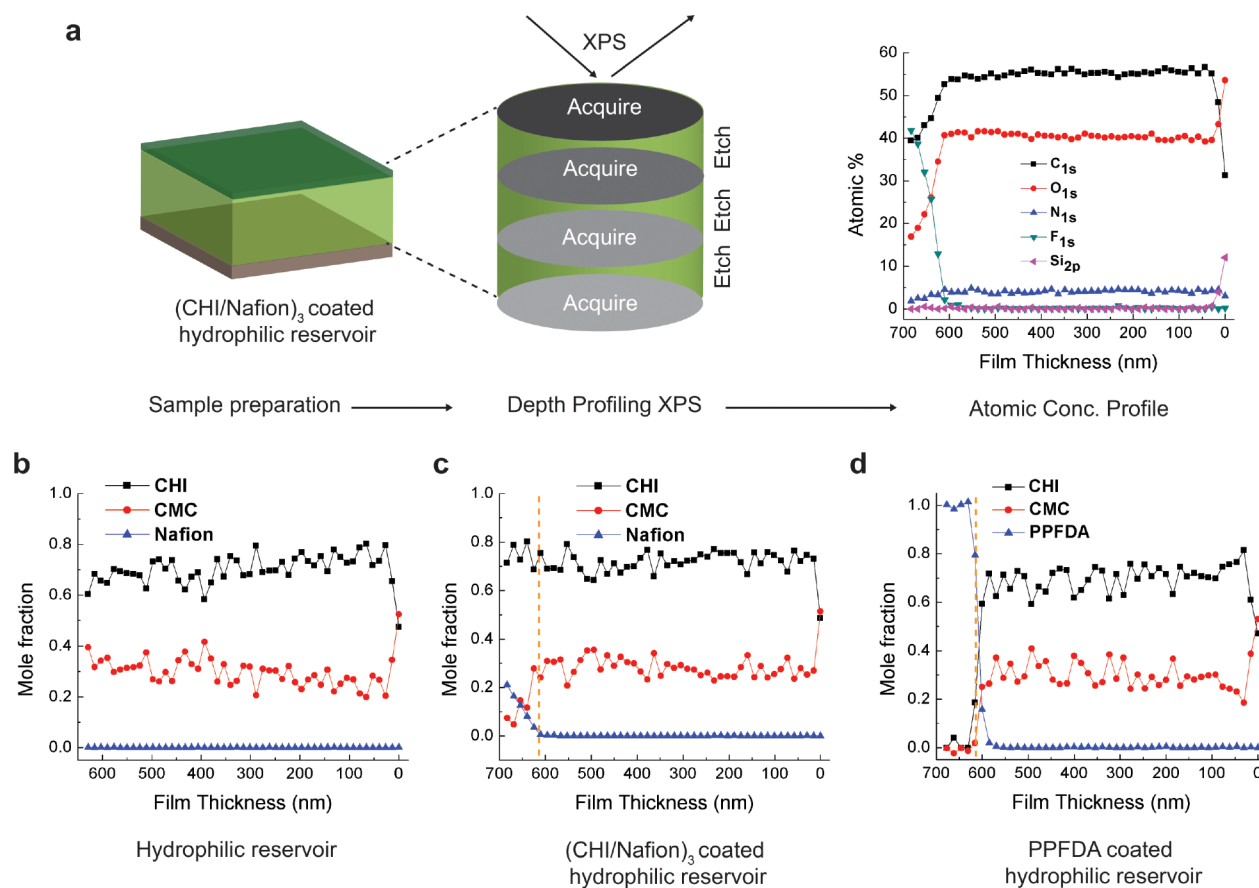
Figure 2. (a) Schematic of C_{60}^+ depth-profiling X-ray photoelectron spectroscopy (XPS) used to acquire atomic concentration profile and molar ratio profile of the various samples tested. Here, the atomic concentration of a $(CHI/Nafion)_3$ coated hydrophilic reservoir is shown as an example. (b) Molar repeat unit ratio of the hydrophilic reservoir $((CHI/CMC)_{30})$ with depth in the film. (c) Molar repeat unit ratio of a $(CHI/Nafion)_3$ coated hydrophilic reservoir with depth in the film. (d) Molar repeat unit ratio of a PPFDA coated hydrophilic reservoir with depth in the film. Orange dotted line represents the film thickness before deposition of a hydrophobic capping layer.

scattering film of water on the surface as shown in Figure 1d. When this hydrophilic film was subsequently coated with multilayers of hydrophobic CHI/Nafion, the film exhibited zwitter-wettable behavior as indicated by the retention of antifogging properties coupled with hydrophobic surface characteristics when exposed to water droplets as shown in Figure 1e. When the same CHI/CMC hydrophilic film was coated with the hydrophobic PPFDA polymer, the multilayer film lost its ability to prevent fog formation. Table 1 shows that the change in film thickness after the addition of the hydrophobic outer layers was essentially the same: 69 and 62 nm, respectively. Both hydrophobic control films, (CHI/Nafion)_30 and PPFDA, exhibited extensive fog formation. Our results clearly show that contact angle measurements alone cannot be used to predict antifog behavior. As shown in more detail below, when water molecules from the vapor are able to permeate rapidly through a hydrophobic capping layer to reach an underlying hydrophilic reservoir, the resultant zwitter-wettable film is able to prevent fogging.

3.2. Axial Composition Analysis Using Depth Profiling X-ray Photoelectron Spectroscopy. Before discussing the water molecule transport properties of the hydrophobic capping layers, it is important to determine if these layers are in fact confined to the surface or penetrating into the underlying hydrophilic reservoir. Interdiffusion of adsorbing layers into heterostructured multilayer thin films is well documented in the literature and can result in dramatic

changes in expected properties.[15−17] Chemical composition analysis normal to the heterostructured film surfaces was performed using C_{60} cluster-ion depth profiling X-ray photo-electron spectroscopy (XPS). Previously, our group has demonstrated that this technique can measure atomic concentration information as well as analyze interlayer diffusion and material exchange in nanostructured polymer thin films with a resolution around 15 nm.[18] Cluster-ion C_{60} etching is much less damaging to polymers than single-ion etching methods commonly used for inorganic materials.[19] As shown in Figure 2a, the depth profiling process uses iterative C_{60}^+ etching and XPS acquisition to probe the atomic concentration profile with depth. The atomic concentration with depth can be further analyzed using a mass balance to determine the molar repeat unit ratio of the various polymers with depth, allowing for the analysis of polymer interlayer diffusion. The depth-dependent molar repeat unit ratio analysis derived from the XPS measurements, indicate that there is a ∼2:1 CHI:CMC molar repeat unit ratio throughout the entire hydrophilic reservoir. Depth profiling XPS can also detect the addition of the thin $(CHI/Nafion)_3$ (Figure 2c) or PPFDA (Figure 2d) hydrophobic layers that were deposited on top of the hydrophilic reservoir. In both cases, it was found that no significant diffusion of the added layers occurred into the hydrophilic reservoir. The thickness of the hydrophobic capping layers measured via depth profiling XPS (∼70 nm) is similar to the profilometry measurements in Table 1. Due to

the lack of significant interlayer diffusion of the hydrophobic coating layers, coupled with the fact that the CHI:CMC ratio of the hydrophilic reservoir is effectively maintained in all films, it is clear that the different antifogging performance can be attributed to the characteristics of the thin capping layer rather than to any changes induced in the underlying hydrophilic multilayers.

3.3. Permeability Measurements Using Quartz Crystal Microbalance with Dissipation Monitoring. With the insight gained from the depth-profiling XPS study, the ability of the nanometer thick hydrophobic capping layers to transport water molecules was investigated by permeability measurements using a quartz crystal microbalance with dissipation monitoring (QCM-D). It has been previously demonstrated that QCM-D enables real-time measurements of water vapor uptake by a thin film with high precision and provides quantitative information on water diffusivity (D), and solubility (S).[12] Quartz crystals coated with various films are introduced into a chamber where the changes in the frequency and dissipation are monitored upon exposure to a steam of humidified nitrogen.

As shown in Figure 3a, the relative change in mass, $(m_t - m_0)/(m_\infty - m_0)$, was measured following a step change in relative humidity from 30% RH to 60% RH for the three samples: (1) a hydrophilic reservoir of $(CHI/CMC)_{30}$, (2) the $(CHI/Nafion)_3$ coated hydrophilic reservoir and (3) $(CHI/Nafion)_{30}$. The relative change in mass was determined by monitoring the film thickness (Supporting Information, Figure S2). Comparing the sorption behavior of these three samples reveals that the $(CHI/Nafion)_{30}$ multilayer film is highly permeable to water vapor and that assembling the ultrathin $(CHI/Nafion)_3$ capping layers onto the hydrophilic reservoir does not measurably hinder water transport, a central requirement for zwitter-wettability.

In the Supporting Information, we discuss one method of extracting rough estimates of water diffusion coefficients (D) from the transient data shown in Figure 3a. When the hydrophilic reservoir is coated with $(CHI/Nafion)_3$, diffusivity (D) increases slightly from 0.27 to 0.32 $\times$ 10^{-10} cm^2 s^{-1} (Supporting Information, Table S2), while solubility (S, obtained from the equilibrium water uptake, $m_\infty - m_0$) slightly decreases from 97.9 to 94.1 (cm^3 STP) per (cm^3 cm Hg). As for the highly diffusive $(CHI/Nafion)_{30}$, the film was too thin (Supporting Information, Figure S2) to determine the diffusivity (D), while solubility (S) is approximately 4-fold less (20.2 (cm^3 STP) per (cm^3 cm Hg)) than that of the other samples tested, as shown in Figure 3b. These results all indicate that water transport to the underlying hydrophilic reservoir is not detectably impaired by adding the (CHI/Nafion) capping layers to the hydrophilic reservoir films.

The (CHI/Nafion) multilayer system without an underlying reservoir does not have sufficient capacity to absorb water, and therefore it fogs after becoming saturated with water, consistent with the antifogging test results in Figure 1c. On the other hand, the low water vapor permeability of the PPDFA hydrophobic capping layer inhibits the transport of water molecules to the hydrophilic reservoir; its surface is eventually overwhelmed by the undiminished supply of water vapor, leading to nucleation of water droplets and fog formation, as illustrated in the top of Figure 3c.

Previously, it has been reported that hydrophobic surfaces retard nucleation and subsequent growth of water droplets compared to hydrophilic surfaces.[20] It is important to point out
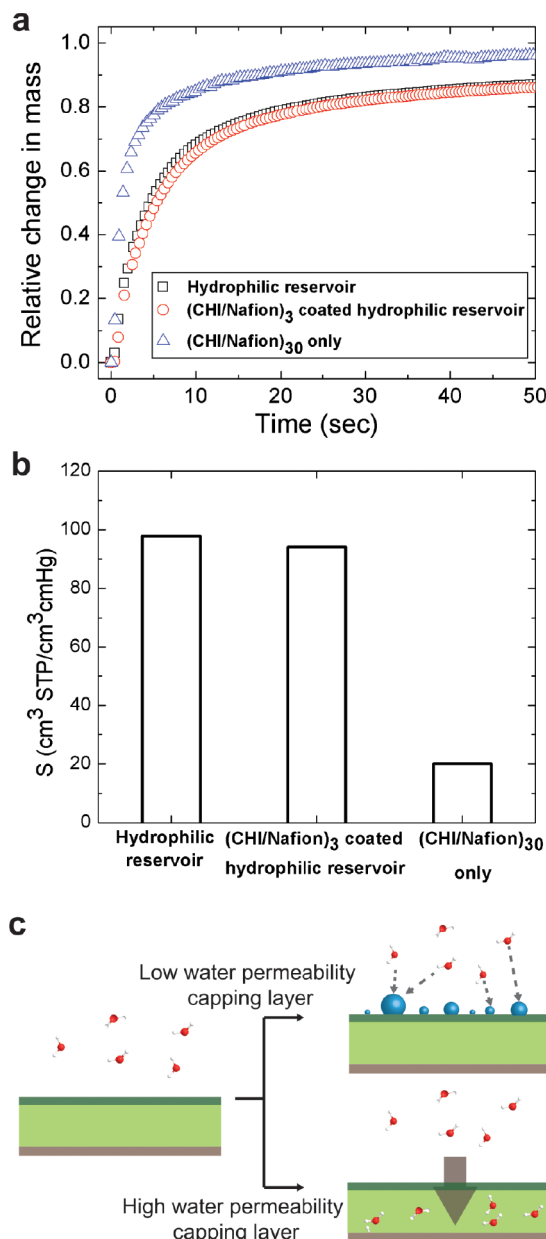

Figure 3. (a) Relative change in mass of a hydrophilic reservoir, $(CHI/Nafion)_3$ coated hydrophilic reservoir, and $(CHI/Nafion)_{30}$ during water sorption (step change in relative humidity from 30% RH to 60% RH). (b) Solubility (S) of water vapor in the hydrophilic reservoir, $(CHI/Nafion)_3$ coated hydrophilic reservoir, and $(CHI/Nafion)_{30}$ (c) Schematic representation of the effect of the ability of a thin hydrophobic capping layer to transport water molecules: For a low water permeability capping layer, water molecules nucleate and grow on the surface while for a high water permeability capping layer, water molecules in the vapor phase prefer to directly imbibe into the underlying hydrophilic reservoir.

that in the antifogging test of Figure 1c, the condensing environment was chosen so that nucleation and subsequent growth of water droplets will occur in any typical hydrophobic sample tested. However, it was only the (CHI/Nafion) coated hydrophilic reservoir that exhibited zwitter-wettability where the surface is hydrophobic to water droplets while highly permeable to water vapor.

3.4. Spatial Control of Water Condensation Using Zwitter-Wettable Films. To demonstrate the unusual
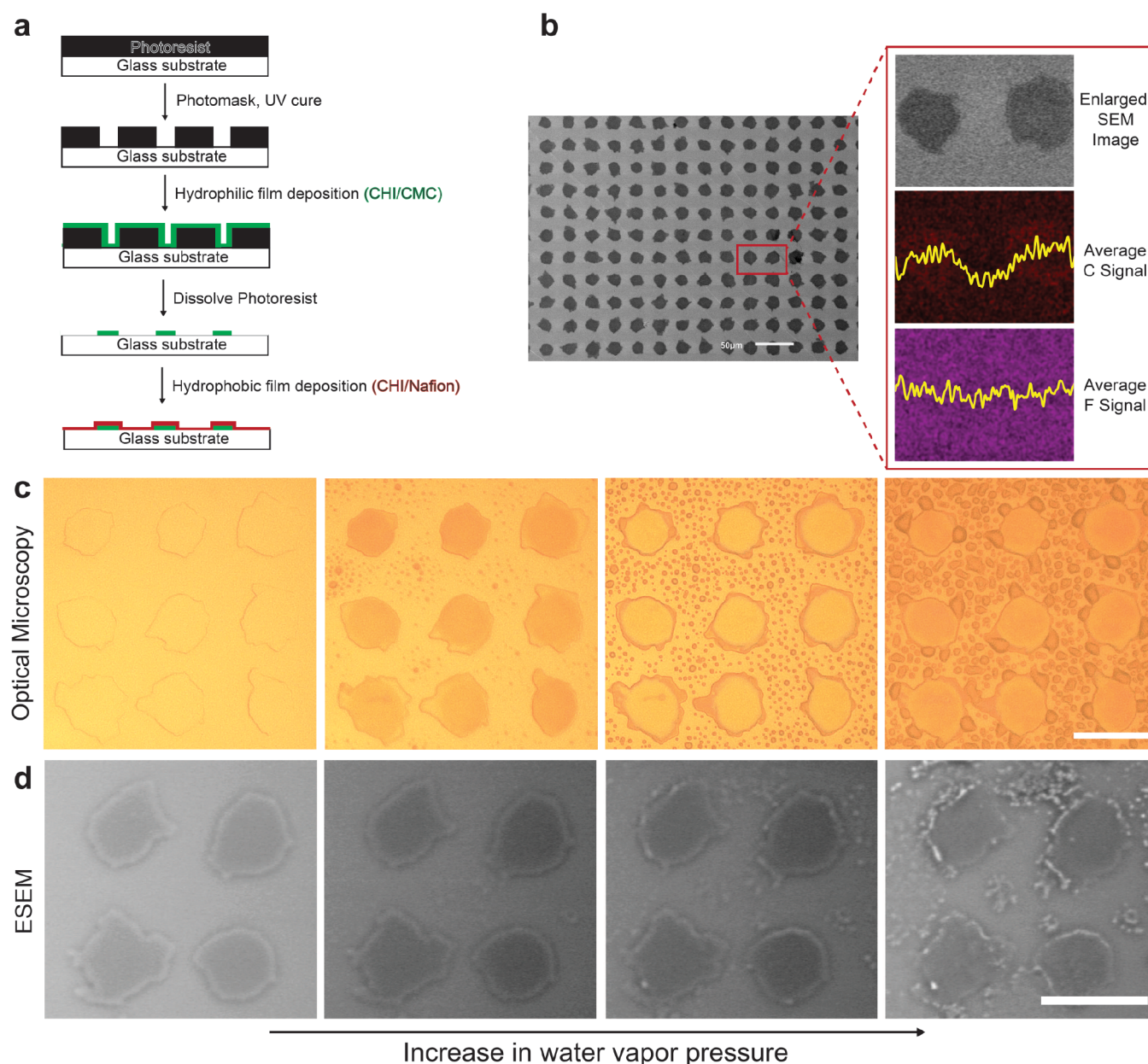
Figure 4. (a) Schematic diagram of the polymer patch fabrication process. (b) Scanning electron microscopy (SEM) image of the polymer patch. Scale bar is 50 μm. Outlet image shows the enlarged SEM image and the average carbon and fluorine signal obtained from energy dispersive X-ray spectrometry (EDS). (c) Optical microscopy image of the polymer patch after exposure to humid air. (d) ESEM images of the condensation of water vapor on a polymer patch. Water droplets start to form on the off-patch areas and at the edges of the patches. Scale bar is 20 μm.

capability of zwitter-wettable films to spatially control condensation of water molecules from the vapor phase, patterned films with zwitter-wettable characteristics were fabricated (Figure 4a). First, patches of the hydrophilic (CHI/CMC) reservoir (10 bilayers) were fabricated using lift-off photolithography.[13,21] 10 bilayers were chosen because higher numbers of bilayers would result in incomplete patterning during the fabrication process. Then, the hydrophobic thin film (CHI/Nafion) (three bilayers) was deposited, resulting in a surface with (CHI/Nafion) over both the small patches of (CHI/CMC) as well as the off-patch areas. The uniform fluorine energy dispersive X-ray spectrometry (EDS) signals (Figure 4b) confirm the coverage of Nafion over the entire area of the substrate, while the nonuniform carbon signal shows the presence of the underlying hydrophilic reservoir

((CHI/CMC)) only in the patterned patch area. When the patterned film is exposed to progressively higher water vapor pressure (Figure 4c,d) the water condensation is spatially controlled. Initially the water diffuses into the hydrophilic reservoir of the patch, changing the refractive index and thus the color of the patch (Figure 4c). As the water vapor pressure increases, droplets form on the interstitial areas, while no droplets are seen on the patch areas with zwitter-wettable characteristics. The capability to spatially control the condensation of water through patterning of the hydrophilic reservoir, while still presenting a uniform hydrophobic surface is indeed unique to zwitter-wettable surfaces; spatial control of the condensation of water molecules has been achieved previously by patterning a surface with significant wettability

contrast to preferentially guide water molecules to nucleate and grow on the hydrophilic regions.[20]

3.5. Surface Wetting Properties of Zwitter-Wettable Films.
Contact angle measurements were performed on the $(CHI/Nafion)_3$ coated hydrophilic reservoir using various probe liquids to further characterize the zwitter-wettable film, as shown in Figure 5. When probed with water, the advancing
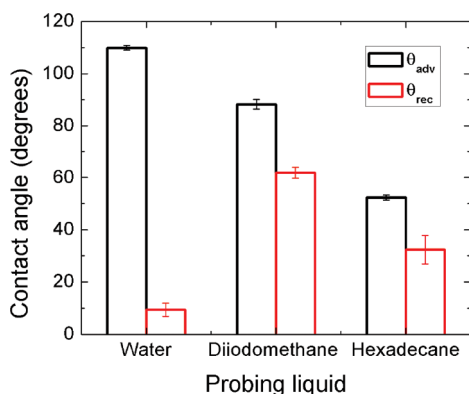

Figure 5. Advancing and receding contact angle of water, diiodomethane and hexadecane on $(CHI/Nafion)_3$ coated hydrophilic reservoir.

contact angle was high ($\sim110°$) while the receding contact angle was only $\sim10°$. Although the significant contact angle hysteresis of water ($\sim100°$) implies that water drops will readily stick on the surface, thorough deliberation of the results presented above reveals that the advancing water contact angle is more critical when considering condensation. At the initial stage of condensation, where there is a competition between nucleation on the surface and permeation of water vapor into the film, the combination of a high water advancing contact angle (i.e., low energy surface) and the highly diffusive nature of the zwitter-wettable film, assures facile permeation of water vapor into the film. As others have seen, a high advancing contact angle is a critical parameter that provides a significantly slower nucleation rate compared to surfaces with a low water advancing contact angle.[20] Furthermore, probing zwitter-wettable films with both high and low surface tension nonpolar liquids, diiodomethane ($\gamma_{LV} = 50.8$ mN/m) and hexadecane ($\gamma_{LV} = 27.5$ mN/m) exhibited advancing contact angles above $50°$ with low contact angle hysteresis ($\sim20°$) similar to the behavior of these two liquids on Teflon (advancing contact angles above $65°$ with contact angle hysteresis of $\sim15°$).[22] Unlike typical hydrophilic films where low surface tension liquids spread completely, zwitter-wettable films have the potential for easy removal of organic contaminants due to the weak retention forces offered by the hydrophobic capping layer.

3.6. Discussion.
The results presented on this model system (not influenced by time dependent surface rearrangement effects) suggest clear design criteria for producing zwitter-wettable films. The basic design should include a strongly hydrophilic reservoir region capped with a nanoscale thin hydrophobic region that is capable of rapidly transporting water molecules from the vapor state into the hydrophilic region. Until now it was thought that surface chemistry and roughness were the main factors for controlling water condensation, but through our analysis we show that a third factor, the capability of a film to transport water molecules needs to be considered for controlling condensation.

4. CONCLUSIONS
In summary, we demonstrated that when a thin hydrophobic layer with sufficient water vapor permeability is assembled on top of a hydrophilic reservoir, zwitter-wettable films with antifogging characteristics can be prepared. Based on depth profiling XPS and QCM-D, the required film properties were detailed for the design of functional zwitter-wettable films. Future work incorporating new surface chemistry and controlled roughness may further extend zwitter-wettable films to enable the fabrication of superhydrophobic antifogging coatings, which remains a technical challenge.[23]

■ ASSOCIATED CONTENT

Ⓢ Supporting Information
Water contact angle evolution over time for various samples tested in this work, change in the thickness of the films during water sorption, detailed XPS depth profiling conditions and analysis of QCM-D mass uptake data. This material is available free of charge via the Internet at http://pubs.acs.org.

■ AUTHOR INFORMATION

Corresponding Authors
*E-mail: rubner@mit.edu (M.F.R).
*E-mail: recohen@mit.edu (R.E.C).

Author Contributions
The paper was written through contributions of all authors. All authors have given approval to the final version of the paper.

Author Contributions
$^{\perp}$These authors contributed equally.

Notes
The authors declare no competing financial interest.

■ ACKNOWLEDGMENTS

■ REFERENCES

(1) Nuraje, N.; Asmatulu, R.; Cohen, R. E.; Rubner, M. F. Durable Antifog Films from Layer-by-Layer Molecularly Blended Hydrophilic Polysaccharides. *Langmuir* **2010**, *27*, 782−791.
(2) Lee, D.; Rubner, M. F.; Cohen, R. E. All-Nanoparticle Thin-Film Coatings. *Nano Lett.* **2006**, *6*, 2305−2312.
(3) Cebeci, F. Ç.; Wu, Z.; Zhai, L.; Cohen, R. E.; Rubner, M. F. Nanoporosity-Driven Superhydrophilicity: A Means to Create Multi-functional Antifogging Coatings. *Langmuir* **2006**, *22*, 2856−2862.
(4) Park, K.-C.; Choi, H. J.; Chang, C.-H.; Cohen, R. E.; McKinley, G. H.; Barbastathis, G. Nanotextured Silica Surfaces with Robust Superhydrophobicity and Omnidirectional Broadband Supertransmissivity. *ACS Nano* **2012**, *6*, 3789−3799.
(5) Briscoe, B. J.; Galvin, K. P. The Effect of Surface Fog on the Transmittance of Light. *Sol. Energy* **1991**, *46*, 191−197.
(6) Lee, H.; Alcaraz, M. L.; Rubner, M. F.; Cohen, R. E. Zwitter-Wettability and Antifogging Coatings with Frost-Resisting Capabilities. *ACS Nano* **2013**, *7*, 2172−2185.

(7) Zhao, J.; Meyer, A.; Ma, L.; Ming, W. Acrylic Coatings with Surprising Antifogging and Frost-Resisting Properties. *Chem. Commun.* **2013**, *49*, 11764−11766.

(8) Hsiao, E.; Barnette, A. L.; Bradley, L. C.; Kim, S. H. Hydrophobic but Hygroscopic Polymer Films − Identifying Interfacial Species and Understanding Water Ingress Behavior. *ACS Appl. Mater. Interfaces* **2011**, *3*, 4236−4241.

(9) Lee, H.; Mensire, R.; Cohen, R. E.; Rubner, M. F. Strategies for Hydrogen Bonding Based Layer-by-Layer Assembly of Poly(vinyl alcohol) with Weak Polyacids. *Macromolecules* **2012**, *45*, 347−355.

(10) Kleingartner, J. A.; Lee, H.; Rubner, M. F.; McKinley, G. H.; Cohen, R. E. Exploring the Kinetics of Switchable Polymer Surfaces with Dynamic Tensiometry. *Soft Matter* **2013**, *9*, 6080−6090.

(11) Paxson, A. T.; Yagüe, J. L.; Gleason, K. K.; Varanasi, K. K. Stable Dropwise Condensation for Enhancing Heat Transfer via the Initiated Chemical Vapor Deposition (iCVD) of Grafted Polymer Films. *Adv. Mater.* **2014**, *26*, 418−423.

(12) Lee, M. H.; Lim, B.; Kim, J. W.; An, E. J.; Lee, D. Effect of Composition on Water Permeability of Model Stratum Corneum Lipid Membranes. *Soft Matter* **2012**, *8*, 1539−1546.

(13) Swiston, A. J.; Cheng, C.; Um, S. H.; Irvine, D. J.; Cohen, R. E.; Rubner, M. F. Surface Functionalization of Living Cells with Multilayer Patches. *Nano Lett.* **2008**, *8*, 4446−4453.

(14) Lee, H.; Sample, C.; Cohen, R. E.; Rubner, M. F. pH-Programmable Sequential Dissolution of Multilayer Stacks of Hydrogen-Bonded Polymers. *ACS Macro Lett.* **2013**, *2*, 924−927.

(15) Lavalle, P.; Vivet, V.; Jessel, N.; Decher, G.; Voegel, J.-C.; Mesini, P. J.; Schaaf, P. Direct Evidence for Vertical Diffusion and Exchange Processes of Polyanions and Polycations in Polyelectrolyte Multilayer Films. *Macromolecules* **2004**, *37*, 1159−1162.

(16) Zacharia, N. S.; Modestino, M.; Hammond, P. T. Factors Influencing the Interdiffusion of Weak Polycations in Multilayers. *Macromolecules* **2007**, *40*, 9523−9528.

(17) Zacharia, N. S.; DeLongchamp, D. M.; Modestino, M.; Hammond, P. T. Controlling Diffusion and Exchange in Layer-by-Layer Assemblies. *Macromolecules* **2007**, *40*, 1598−1603.

(18) Gilbert, J. B.; Rubner, M. F.; Cohen, R. E. Depth-Profiling X-ray Photoelectron Spectroscopy (XPS) Analysis of Interlayer Diffusion in Polyelectrolyte Multilayers. *Proc. Natl. Acad. Sci. U. S. A.* **2013**, *110*, 6651−6.

(19) Sanada, N.; Yamamoto, A.; Oiwa, R.; Ohashi, Y. Extremely Low Sputtering Degradation of Polytetrafluoroethylene by C60 Ion Beam Applied in XPS Analysis. *Surf. Interface Anal.* **2004**, *36*, 280−282.

(20) Varanasi, K. K.; Hsu, M.; Bhate, N.; Yang, W.; Deng, T. Spatial Control in the Heterogeneous Nucleation of Water. *Appl. Phys. Lett.* **2009**, *95*, 094101.

(21) Doshi, N.; Swiston, A.; Gilbert, J. B.; Alcaraz, M.; Cohen, R.; Rubner, M.; Mitragotri, S. Cell-based Drug Delivery Devices Using Phagocytosis-Resistant Backpacks. *Adv. Mater.* **2011**, *23*, H105−H109.

(22) Meuler, A. J.; Chhatre, S. S.; Nieves, A. R.; Mabry, J. M.; Cohen, R. E.; McKinley, G. H. Examination of Wettability and Surface Energy in Fluorodecyl POSS/Polymer Blends. *Soft Matter* **2011**, *7*, 10122−10134.

(23) Gao, X.; Yan, X.; Yao, X.; Xu, L.; Zhang, K.; Zhang, J.; Yang, B.; Jiang, L. The Dry-Style Antifogging Properties of Mosquito Compound Eyes and Artificial Analogues Prepared by Soft Lithography. *Adv. Mater.* **2007**, *19*, 2213−2217.